Phytochemistry 167 (2019) 112085

Contents lists available at ScienceDirect

Phytochemistry

journal homepage: www.elsevier.com/locate/phytochem

Phenolic constituents from the twigs of *Betula schmidtii* collected in Goesan, Korea

Kyoung Jin Park[a], Joon Min Cha[a], Lalita Subedi[b,c], Sun Yeou Kim[b,c], Kang Ro Lee[a,*]

[a] Natural Products Laboratory, School of Pharmacy, Sungkyunkwan University, Suwon, 16419, Republic of Korea
[b] Gachon Institute of Pharmaceutical Science, Gachon University, Incheon, 21936, Republic of Korea
[c] College of Pharmacy, Gachon University, 191 Hambakmoero, Yeonsu-gu, Incheon, 21936, Republic of Korea

ARTICLE INFO

Keywords:
Betula schmidtii Regel
Betulaceae
Phenolic derivatives
Anti-inflammatory activity

ABSTRACT

Six undescribed phenolic derivatives along with thirty two known compounds were isolated from the twigs of *Betula schmidtii*. The chemical structures were characterized through extensive spectroscopic analysis and chemical methods. All known compounds were first isolated in this plant. The anti-inflammatory effect of the isolates was tested by measuring nitric oxide production in lipopolysaccharide-activated BV-2 cells. Isotachioside, 4-allyl-2-hydrophenyl 1-*O*-*β*-D-apiosyl-(1 → 6)-*β*-D-glucopyranoside, genistein 5-*O*-*β*-D-glucoside, and prunetinoside showed a slight potency to lower the NO production against LPS-activated microglia with IC_{50} values of 23.9, 25.3, 28.8, and 34.0 μM, respectively.

1. Introduction

Inflammation in the central nervous system (CNS) is termed as neuroinflammation. Neuroinflammation cause degeneration and death of neurons characterizing by neurodegenerative conditions like Alzheimer's disease (AD), Parkinson's disease (PD), ischemia, and multiple sclerosis (MS) (Gelders et al., 2018). CNS immune cells specially microglia play a key role for the neuroinflammation through its chronic activation and subsequent overproduction of inflammatory mediators including nitric oxide (NO) (Lull and Block, 2010). Excessive production of NO by activated microglia as a characteristic feature of neuroinflammation is known to be a major reason behind pathogenesis of neurodegenerative disorders like AD, PD, MS, and ischemia etc. (Yuste et al., 2015).

Betula genus, the largest group of Betulaceae, consists of 137 species distributed widely in areas of mild climate in the northern hemisphere. They have been commonly used as traditional medicines to treat arthritis, rheumatism, and renal disease in different regions of the world. Previous studies of this genus have reported chemical constituents including triterpenoids, diarylheptanoids, phenylbutanoids, flavonoids, lignans, and phenolic compounds associated with anticancer, anti-inflammatory, arthritis, rheumatism, antioxidant, antimicrobial, and antiviral activities. However, *Betula schmidtii* Regel has rarely been investigated for potential bioactive chemical constituents due to its localized distribution in Northeast Asia (Rastogi et al., 2015; Fuchino et al., 1998). Hence, a phytochemical research of *B. schmidtii* twigs was conducted. Following our previous report of triterpenoids from the $CHCl_3$ layer of a *B. schmidtii* MeOH extract (Park et al., 2018), thirty eight phenolic derivatives including four undescribed phenolic glycosides (**1**–**4**), an undescribed lignan glycoside (**20**), and an undescribed isoflavonoid glycoside (**28**) were further isolated and identified from the EtOAc and *n*-BuOH layers (Fig. 1). Herein, the isolation and structural elucidation of compounds **1**–**38** and their inhibitory activity of NO generation are presented.

2. Results and discussion

Compound **1**, a colorless gum, was established as $C_{19}H_{20}O_9$ on the basis of its HRESIMS data (*m/z* 415.1004, $[M + Na]^+$). The ^1H NMR data displayed the presence of one monosubstituted aromatic ring [δ_H 8.08 (2H, dd, J = 8.3, 1.2 Hz, H-2″ and H-6″), 7.61 (1H, t, J = 7.5 Hz, H-4″), and 7.49 (2H, brt, J = 7.5 Hz, H-3″ and H-5″)], one 1,3,5-trisubstituted aromatic ring [δ_H 6.13 (2H, d, J = 2.1 Hz, H-2 and H-6) and 6.00 (1H, t, J = 2.1 Hz, H-4)], and one glucopyranosyl unit [δ_H 4.92 (1H, d, J = 7.6 Hz, H-1′), 4.76 (1H, dd, J = 11.8, 2,2 Hz, H-6′a), 4.34 (1H, dd, J = 11.8, 7.2 Hz, H-6′b), 3,79 (1H, ddd, J = 9.5, 7.2, 2.2 Hz, H-5′), 3.52 (1H, m, H-3′), 3.48 (1H, m, H-2′), and 3.46 (1H, m, H-4′)]. The ^{13}C NMR data showed 15 peaks for 19 carbons, including one carbonyl carbon [δ_C 168.2 (C-7″)], two aromatic rings [δ_C 160.9 (C-1), 160.3 (C-3 and C-5), 134.3 (C-4″), 131.3 (C-1″), 130.9 (C-2″ and C-6″)

* Corresponding author. Natural Products Laboratory, School of Pharmacy, Sungkyunkwan University, 2066 Seobu-ro, Jangan-gu, Suwon, 16419, Republic of Korea.
E-mail address: krlee@skku.edu (K.R. Lee).

https://doi.org/10.1016/j.phytochem.2019.112085
Received 11 June 2019; Received in revised form 6 August 2019; Accepted 6 August 2019

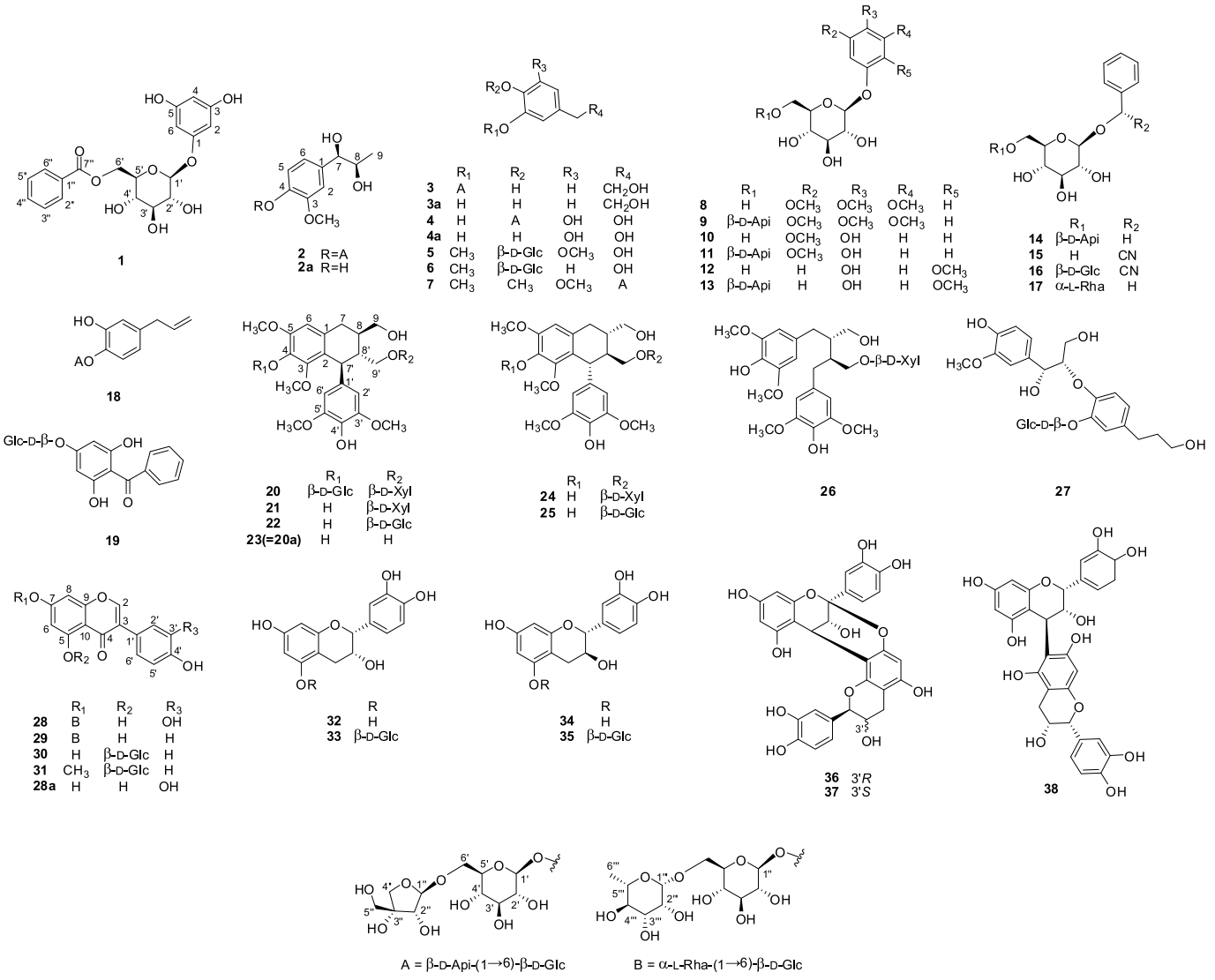

Fig. 1. Chemical structures of compounds **1**–**38**.

129.7 (C-3″ and C-5″), 98.1 (C-4), and 96.8 (C-2 and C-6)], and one anomeric carbon [δ_C 102.0 (C-1′)]. Analysis of these 1D NMR data of **1** (Table 1) indicated similarities with those of 3,4-dihydroxyphenyl-(6′-*O*-benzoyl)-*O*-*β*-D-glucopyranoside (Verotta et al., 1999). The major difference was in the presence of a 1,3,5-trisubstituted benzene ring in **1**, instead of a 1,3,4-trisubstituted benzene ring in 3,4-dihydroxyphenyl-(6′-*O*-benzoyl)-*O*-*β*-D-glucopyranoside. The planar structure of **1** was determined from 2D NMR (COSY, HSQC, and HMBC) spectroscopic data (Fig. 2). The HMBC correlations of H-1′/C-1 and H-6′/C-7″ indicated the location of the glucopyranosyl moiety and benzoic acid, respectively. The coupling constant of the anomeric proton (J = 7.6 Hz) confirmed as *β*-glucopyranose (Kim et al., 2015) and acid hydrolysis of **1** gave a D-glucopyranose, which was identified by co-TLC confirmation and GC/MS analysis (Hara et al., 1987). Thus, the structure of **1** was elucidated as 3,5-dihydroxyphenyl-(6′-*O*-benzoyl)-1-*O*-*β*-D-glucopyranoside.

Compound **2**, colorless gum, gave the molecular formula $C_{21}H_{32}O_{13}$, based on the pseudomolecular ion peak at *m/z* 515.1735 (calcd for $C_{21}H_{32}O_{13}Na$, 515.1741). The 1D NMR data (Table 1) were closely similar to those of 1-(4-hydroxy-3-methoxyphenyl)propan-1,2-diol isolated from *Zingiber officinale* (Ma et al., 2004), except for the additional presence of apiose signals [δ_H 4.96 (1H, d, J = 2.4 Hz, H-1″), 3.95 (1H, d, J = 9.7 Hz, H-4″a), 3.88 (1H, d, J = 2.4 Hz, H-2″), 3.74 (1H, d, J = 9.7 Hz, H-4″b), and 3.57 (2H, brs, H-5″); δ_C 111.1 (C-1″), 80.7 (C-3″), 78.1 (C-2″), 75.1 (C-4″), and 65.7 (C-5″)] and glucose signals [δ_H 4.83 (1H, d, J = 7.4 Hz, H-1′), 3.99 (1H, dd, J = 11.1, 1.7 Hz, H-6′a), 3.61 (1H, dd, J = 11.1, 6.6 Hz, H-6′b), 3.54 (1H, m, H-5′), 3.48 (1H, m, H-2′), 3.43 (1H, m, H-3′), and 3.35 (1H, m, H-4′); δ_C 103.0 (C-1′), 77.9 (C-3′), 77.2 (C-5′), 75.0 (C-2′), 71.7 (C-4′), and 68.8 (C-6′)]. The large coupling constant of H-1′ (J = 7.4 Hz) and the small coupling constant of H-1″ (J = 2.4 Hz) indicated a *β*-glucopyranose and a *β*-apiofuranose, respectively (Kim et al., 2015; Kanchanapoom et al., 2002). On the basis of the HMBC data, the correlation of H-1″/C-6′ was confirmed, indicating that *β*-apiofuranose was connected with C-6′ of *β*-glucopyranose. The disaccharide moiety of **2** was established to be located at C-4 by the HMBC correlation of H-1′/C-4. Additionally, the location of a methoxy group at C-3 was corroborated from the HMBC cross-peak between OCH_3-3 and C-3 (Fig. 2). D-Glucopyranose and D-apiofuranose acquired via acid hydrolysis of **2** were established by co-TLC confirmation and GC/MS analysis (Hara et al., 1987). The relative configuration at C-7 and C-8 of **2** was confirmed by their coupling constant. The large coupling constant of the H-7 (J = 6.8 Hz) indicated that C-7 and C-8 were to be *threo*-form (Balboul et al., 1996). The absolute configuration of **2** was determined through comparison of the optical rotation of **2a** {$[\alpha]_D^{25}$–47.4 (*c* 0.05, MeOH)} as 7*R*, 8*R* (Lee and Ley, 2003). Hence, the structure of **2** was established as (7*R*,8*R*)-1-(4-

Table 1
^{1}H NMR [ppm, mult, (J in Hz)] and^{13}C NMR data of compounds **1**–**4** in CD_3OD.

Position	1		2		3		4	
	δ_H	δ_C	δ_H	δ_C	δ_H	δ_C	δ_H	δ_C
1		160.9		138.5		132.1		140.9
2	6.13 d (2.1)	96.8	7.03 d (1.8)	112.6	7.08 d (1.8)	119.8	6.42 brs	107.4
3		160.3		150.8		146.8		151.4
4	6.00 t (2.1)	98.1		147.5		146.7		133.8
5		160.3	7.13 d (8.3)	117.9	6.76 d (8.2)	117.1		151.4
6	6.13 d (2.1)	96.8	6.91 dd (8.3, 1.8)	121.2	6.79 dd (8.2, 1.8)	125.3	6.42 brs	107.4
7			4.31 d (6.8)	80.0	2.73 t (7.2) (2H)	39.8	4.43 s (2H)	65.0
8			3.80 m	72.9	3.71 t (7.2) (2H)	64.6		
9			0.99 d (6.4) (3H)	19.4				
1′	4.92 d (7.6)	102.0	4.83 d (7.4)	103.0	4.71 d (7.5)	104.6	4.54 d (7.8)	107.9
2′	3.48 m	74.9	3.48 m	75.0	3.48 m	75.0	3.48 m	75.0
3′	3.52 m	78.1	3.43 m	77.9	3.45 m	77.7	3.41 m	77.7
4′	3.46 m	72.5	3.35 m	71.7	3.35 m	71.7	3.39 m	71.4
5′	3.79 ddd (9.5, 7.2, 2.2)	75.6	3.54 m	77.2	3.56 m	77.3	3.51 m	77.5
6′	4.76 dd (11.8, 2.2)	65.7	3.99 dd (11.1, 1.7)	68.8	4.05 dd (10.5, 1.4)	68.8	3.98 dd (11.1, 2.2)	68.6
	4.34 dd (11.8, 7.2)		3.61 dd (11.1, 6.6)		3.60 dd (10.5, 6.7)		3.67 dd (11.1, 6.1)	
1″		131.3	4.96 d (2.4)	111.1	5.00 d (2.5)	111.1	4.99 d (2.3)	111.2
2″	8.08 dd (8.3, 1.2)	130.9	3.88 d (2.4)	78.1	3.96 d (2.5)	78.2	3.93 d (2.3)	78.3
3″	7.49 brt (7.5)	129.7		80.7		80.6		80.7
4″	7.61 t (7.5)	134.3	3.95 d (9.7)	75.1	3.98 d (9.7)	75.1	3.97 d (9.7)	75.2
			3.74 d (9.7)		3.77 d (9.7)		3.76 d (9.7)	
5″	7.49 brt (7.5)	129.7	3.57 brs (2H)	65.7	3.59 d (1.1) (2H)	65.6	3.60 brs (2H)	65.9
6″	8.08 dd (8.3, 1.2)	130.9						
7″		168.2						
3-OCH_3			3.88 s (3H)	56.8				

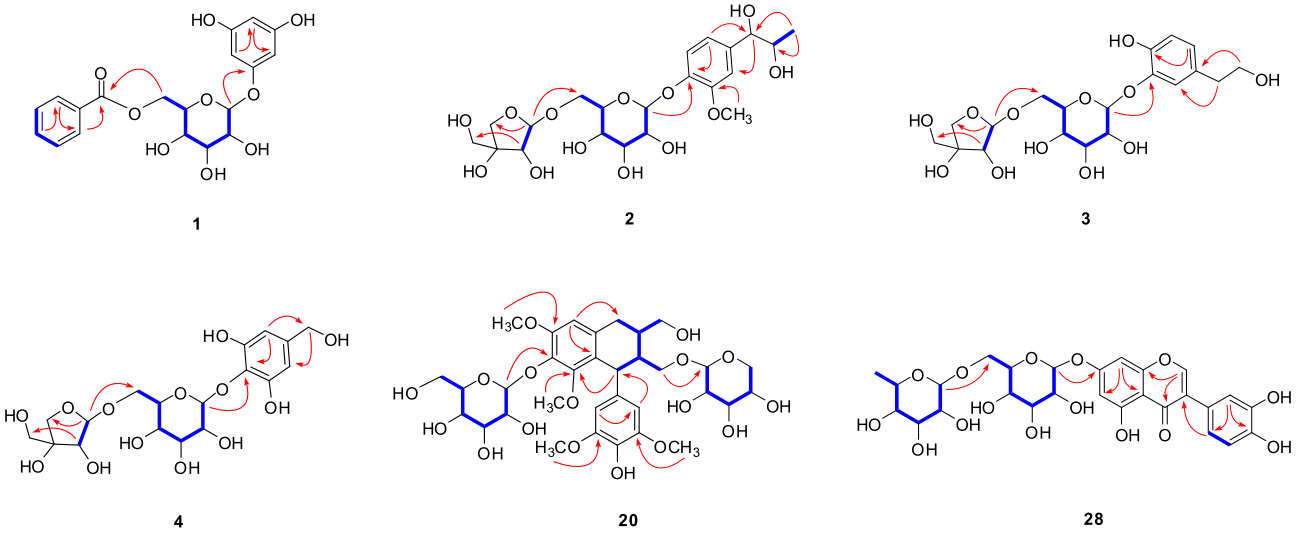

Fig. 2. Key COSY (bold) and HMBC (arrow) correlations of **1**–**4**, **20**, and **28**.

hydroxy-3-methoxyphenyl)propan-7,8-diol-4-*O*-*β*-D-apiofuranosyl-(1 → 6)-*O*-*β*-D-glucopyranoside. Compound **3** was obtained as a colorless gum, and its molecular formula was confirmed as $C_{19}H_{28}O_{12}$ based on the HRESIMS, displaying a pseudomolecular ion peak $[M + Na]^+$ at m/z 471.1473 (calcd for $C_{19}H_{28}O_{12}Na$, 471.1478). The ^{1}H and ^{13}C NMR spectra of **3** were quite similar to those of 2-hydroxy-5-(2-hydroxyethyl)phenyl *O*-*α*-D-apiofuranosyl-(1 → 6)-*O*-*β*-D-glucopyranoside (Lei et al., 2008), except for the coupling constant of H-1″ (J = 2.5 Hz) and chemical shifts of C-1″ (δ_C 111.1) (Table 1), indicating the *β* configuration of apiofuranosyl unity in **3**. The HMBC correlation from H-1″ to C-6′ revealed the linkage between two sugars and correlation from H-1′ to C-3 established the position of the disaccharide moiety (Fig. 2). The sugar analysis of **3** was confirmed using a same approach to that of **2**. Thus, the structure of **3** was determined as 4-hydroxy-1-(2-hydroxyethyl)phenyl-3-*O*-*β*-D-apiofuranosyl-(1 → 6)-*O*-*β*-D-glucopyranoside.

Compound **4** was purified as a colorless gum with the molecular formula of $C_{18}H_{26}O_{13}$. The molecular formula was deduced by the positive ion peak $[M + Na]^+$ in the HRESIMS. The ^{1}H and ^{13}C NMR data of **4** (Table 1) were very similar to those of 6′-*O*-*β*-D-apiofuranosylcalleryanin (Itoh et al., 2008). The major difference was found to be the presence of a hydroxyl group at C-5 of aromatic ring [δ_H 6.42 (2H, brs, H-2 and H-6); δ_C 151.4 (C-3 and C-5), 140.9 (C-1), 133.8 (C-4), and 107.4 (C-2 and C-6)], indicating that **4** has a 1,3,4,5-tetrasubstituted aromatic ring. The HMBC cross-peaks of H-1′/C-4 and H-1″/C-6′ confirmed the connection between glucopyranosyl moiety with the aglycone and the apiofuranosyl moiety (Fig. 2). Acid hydrolysis of **4** yielded two sugar moieties, which were determined by the identical manner to that of **2**. Therefore, compound **4** was established as 3,5-dihydroxy-1-(hydroxymethyl)phenyl-4-*O*-*β*-D-apiofuranosyl-(1 → 6)-*O*-*β*-D-glucopyranoside.

The molecular formula of compound **20** was confirmed as $C_{33}H_{46}O_{17}$ from positive ion HRESIMS and ^{13}C NMR data. The ^{1}H and

Table 2
^{1}H NMR [ppm, mult, (*J* in Hz)] and^{13}C NMR data of compounds **20** and **28** in CD_3OD.

Position	20		28	
	δ_H	δ_C	δ_H	δ_C
1		134.8		
2		125.5	8.18 brs	155.8
3		151.6		125.1
4		137.2		182.6
5		151.6		163.5
6	6.70 s	107.9	6.50 brs	101.4
7	2.78 dd (15.4, 4.7) 2.67 dd (15.4, 11.6)	32.6		164.7
8	1.71 m	38.9	6.74 brs	96.0
9	3.64 m 3.56 dd (10.9, 6.5)	64.5		159.3
10				108.2
1′		137.5		123.9
2′	6.44 brs	105.5	7.05 brs	117.5
3′		147.6		146.4
4′		133.2		147.0
5′		147.6	6.82 brd (7.4)	116.4
6′	6.44 brs	105.5	6.88 brd (7.4)	121.8
7′	4.44 d (6.3)	41.4		
8′	2.12 m	45.1		
9′	3.83 dd (9.6, 5.6) 3.44 m	69.5		
1″	4.24 d (7.5)	104.0	4.98 d (6.2)	101.8
2″	3.24 dd (9.0, 7.6)	73.5	3.50 brs	74.8
3″	3.33 overlap	76.6	3.49 brs	78.2
4″	3.49 m	69.8	3.34 m	71.8
5″	3.84 dd (11.4, 5.4) 3.18 dd (11.4, 10.3)	65.5	3.64 m	77.3
6″			4.08 d (10.6) 3.56 m	68.0
1‴	4.91 d (7.4)	103.3	4.70 brs	102.4
2‴	3.46 m	74.3	3.90 brs	72.2
3‴	3.18 m	76.8	3.78 m	72.6
4‴	3.40 m	69.8	3.37 m	74.3
5‴	3.41 m	76.4	3.67 m	70.0
6‴	3.72 dd (12.0, 2.4) 3.64 m	61.0	1.22 d (6.2) (3H)	18.1
5-OCH_3	3.40 s	60.0		
7-OCH_3	3.88 s	55.5		
3′,5′-OCH_3	3.77 s	55.4		

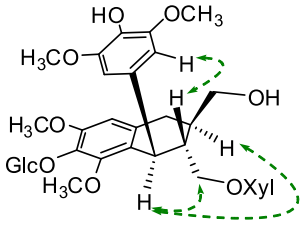

20

Fig. 3. Key NOESY correlations of **20**.

^{13}C NMR spectra (Table 2) closely resembled those of lyoniside (**21**) (Smite et al., 1995), except for the presence of glucose signals [δ_H 4.91 (1H, d, *J* = 7.4 Hz, H-1‴), 3.72 (1H, dd, *J* = 12.0, 2.4 Hz, H-6‴a), 3.64 (1H, m, H-6‴b), 3.46 (1H, m, H-2‴), 3.41 (1H, m, H-5‴), 3.40 (1H, m, H-4‴), and 3.18 (1H, m, H-3‴); δ_C 103.3 (C-1‴), 76.8 (C-3‴), 76.4 (C-5‴), 74.3 (C-2‴), 69.8 (C-4‴), and 61.0 (C-6‴)]. The configurations of sugars indicated *β*-xylopyranose and *β*-glucopyranose based on the *J* values of anomeric protons [*J* = 7.5 Hz (H-1″) and *J* = 7.4 Hz (H-1‴)], respectively (Smite et al., 1995). The HMBC correlation between H-1‴ and C-4 indicated that the *β*-glucopyranosyl unit is connected to C-4. Acid hydrolysis of **20** gave (+)-lyoniresinol (**20a**), identified by ^{1}H NMR and positive specific rotation {$[\alpha]_D^{25}$ + 58.2 (*c* 0.03, MeOH)} (Li and Seeram, 2010). The D configuration of glucopyranosyl and xylopyranosyl units in compound **20** was determined using the method described for **2**, respectively. The relative configuration was confirmed via NOESY correlations of H-2/H-4 and H-3/H-2′ and 6′, and the 8*R*, 7′*S*, 8′*R* configuration was deduced from the positive Cotton effects at 241 and 272 nm by comparison of the CD spectrum (Fig. 3 and Fig. S32, Supplementary material) (Suh et al., 2015). Therefore, compound **20** was elucidated as (+)-(8*R*,7′*S*,8′*R*)-6-*O*-*β*-D-glucopyranosyl lyoniresinol-9′-*O*-*β*-D-xylopyranoside.

Compound **28** was isolated as a yellowish gum with a molecular formula of $C_{27}H_{30}O_{15}$ established using HRESIMS data. Inspection of the NMR data of **28** (Table 2) was quite similar to those of sphaerobioside (**29**) (Laupattarakasem et al., 2004), with the main difference being that the signals of a 1′,3′,4′-trisubstituted aromatic ring [δ_H 7.05 (1H, brs, H-2′), 6.88 (1H, brd, *J* = 7.4 Hz, H-6′), and 6.82 (1H, brd, *J* = 7.4 Hz, H-5′); δ_C 147.0 (C-4′), 146.4 (C-3′), 123.9 (C-1′), 121.8 (C-6′), and 116.4 (C-5′)], instead of a 1′,4′-disubstituted aromatic ring found in **29**. The coupling constants of anomeric protons [δ_H 4.98 (1H, d, *J* = 6.2 Hz, H-1″) and 3.90 (1H, brs, H-1‴)] indicated the configuration of *β*-glucopyranose and *α*-rhamnopyranose, respectively (Laupattarakasem et al., 2004).The HMBC cross-peaks of H-1‴/C-6″ and H-1″/C-7 confirmed the position and presence of a rutinose [*α*-rhamnopyranosyl-(1 → 6)-*β*-glucopyranoside] moiety (Fig. 2). Acid hydrolysis of **28** yielded the aglycone, which was identified as orobol (**28a**) (Anhut et al., 1984) by comparing its ^{1}H NMR spectrum data, together with D-glucopyranose and L-rhamnopyranose, which were confirmed by GC/MS analysis, respectively (Hara et al., 1987). Thus, compound **28** was determined as orobol-7-*O*-*α*-L-rhamnopyranosyl-(1 → 6)-*O*-*β*-D-glucopyranoside.

The isolated 32 known compounds were identified as 3,5-dimethoxy-4-hydroxybenzyl alcohol 4-*O*-*β*-D-glucopyranoside (**5**) (Kitajima et al., 1998), vanillyl alcohol 4-*O*-*β*-D-glucopyranoside (**6**) (Kanho et al., 2005), apionikoenoside (**7**) (Matsuoka et al., 2011), 3,4,5-trimethoxyphenol *O*-*β*-D-glucopyranoside (**8**) (Le et al., 2012), 3,4,5-trimethoxyphenol *O*-*β*-D-apiofuranosyl-(1 → 6)-*β*-D-glucopyranoside (**9**) (Fuchino et al., 1995), isotachioside (**10**) (Zhong et al., 1999), 4-hydroxy-3-methoxyphenol *O*-*β*-D-apiopyranosyl (1 → 6)-*O*-*β*-D-glucopyranoside (**11**) (Kitajima et al., 2003), tachioside (Zhong et al., 1999) (**12**), canthoside D (**13**) (Kanchanapoom et al., 2002), benzyl 6-*O*-*β*-D-apiofuranosyl-*β*-D-glucopyranoside (**14**) (Suzuki et al., 1988), prunasin (**15**) (Seigler et al., 2002), amygdalin (**16**) (Backheet et al., 2003), benzyl *O*-*α*-L-rhamnopyranosyl-(1 → 6)-*β*-D-glucopyranoside (**17**) (Kawahara et al., 2005), 4-allyl-2-hydrophenyl 1-*O*-*β*-D-apiosyl-(1 → 6)-*β*-D-glucopyranoside (**18**) (Yamauchi et al., 2007), 2,6-dihydroxy-4-*O*-*β*-D-glucopyranosylbenzophenone (**19**) (Fu et al., 2011), lyoniside (**21**) (Smite et al., 1995), (+)-lyoniresinol-3*α*-*O*-*β*-D-glucopyranoside (**22**) (Lee et al., 2005), (+)-lyoniresinol (**23**) (Li and Seeram, 2010), nudiposide (**24**) (Smite et al., 1995), (−)-lyoniresinol-3*α*-*O*-*β*-D-glucopyranoside (**25**) (Achenbach et al., 1992), ssioriside (**26**) (Yoshinari et al., 1989), (−)-(7*R*,8*S*)-4,7,9,3′,9′-pentahydroxy-3-methoxy-8-4′-oxyneolignan-3′-*O*-*β*-D-glucopyranoside (**27**) (Gan et al., 2008), sphaerobioside (**29**) (Laupattarakasem et al., 2004), genistein 5-*O*-*β*-D-glucoside (**30**) (Geibel et al., 1990), prunetinoside (**31**) (Khalid et al., 1989), (−)-epicatechin (**32**) (Abdel Kader Ahmed and Al-Refai, 2014), (−)-epicatechin 5-*O*-*β*-D-glucopyranoside (**33**) (Cui et al., 1992b), (+)-catechin (**34**) (Abdel Kader Ahmed and Al-Refai, 2014), (+)-catechin 5-*O*-*β*-D-glucopyranoside (**35**) (Raab et al., 2010), proanthocyanidin A-2 (**36**) (Lou et al., 1999), proanthocyanidin A-1 (**37**) (Lou et al., 1999), and procyanidin B-5 (**38**) (Cui et al., 1992a) by comparison with NMR and MS data in the literature.

In this study, NO production assay was performed to evaluate the anti-inflammatory effect of isolates (**1–38**) against LPS-activated murine microglia (Table 3). Compound **10** (IC_{50} 23.9 μM) showed more potent effect than the positive control, N^G-mono-methyl-L-arginine (L-NMMA) (IC_{50} 25.2 μM). Besides, compounds **18**, **30**, and **31** displayed

Table 3
Inhibitory effect of compounds **1**–**38** on NO production in LPS-activated BV-2 cells.

Comp.	IC_{50} (μM)[a]	Cell Viability (%)[b]	Comp.	IC_{50} (μM)[a]	Cell Viability (%)[b]
1	66.7	89.6 ± 2.0	**21**	85.3	94.3 ± 3.4
2	55.6	106.5 ± 15.6	**22**	132.6	98.0 ± 5.2
3	130.6	101.9 ± 5.5	**23**	48.8	103.9 ± 6.0
4	44.8	103.0 ± 12.8	**24**	39.9	97.6 ± 2.3
5	58.4	101.9 ± 9.0	**25**	> 500	104.0 ± 5.5
6	62.0	108.9 ± 9.7	**26**	201.4	95.6 ± 4.9
7	45.1	90.6 ± 2.9	**27**	96.6	130.3 ± 3.9
8	54.1	93.4 ± 7.2	**28**	> 500	111.1 ± 9.5
9	51.5	93.8 ± 9.2	**29**	37.9	91.6 ± 7.1
10	23.9	114.1 ± 5.4	**30**	28.8	93.6 ± 9.5
11	46.2	95.7 ± 15.7	**31**	34.1	98.7 ± 6.9
12	53.1	99.8 ± 6.0	**32**	> 500	104.7 ± 11.5
13	39.0	93.8 ± 5.0	**33**	81.0	89.9 ± 6.5
14	49.1	86.4 ± 4.8	**34**	69.7	102.9 ± 3.8
15	72.0	93.4 ± 5.4	**35**	41.2	94.2 ± 2.8
16	103.1	88.2 ± 2.5	**36**	> 500	88.0 ± 3.8
17	45.6	102.4 ± 6.5	**37**	62.6	94.0 ± 5.7
18	25.3	96.0 ± 6.4	**38**	74.8	101.0 ± 11.7
19	44.4	99.5 ± 14.6	L-NMMA[c]	25.2	105.2 ± 2.6
20	93.8	100.9 ± 15.4			

[a] IC_{50} value of each compound was defined as the concentration (μM) that caused 50% inhibition of NO production in LPS-activated BV-2 cells.
[b] Cell viability after treatment with 20 μM of each compound was determined by the MTT assay and is expressed as a percentage (%). Results are means of three independent experiments, and the data are expressed as mean ± SD.
[c] L-NMMA as a positive control.

moderate effects with IC_{50} values of 25.3, 28.8, and 34.0 μM, respectively. Other compounds showed weak or no activity to lower the NO production against LPS-activated microglia. None of the treated compounds showed any significant toxicity to the microglial cell up to the concentration of 20 μM.

3. Conclusion

A phytochemical study on the MeOH extract of the twigs of *B. schmidtii* led to the isolation of 38 phenolic derivatives including six previously undescribed compounds (**1**–**4**, **20**, and **28**). Their chemical structures were elucidated by spectroscopic and spectrometric methods, and all the known compounds (**5**–**19**, **21**–**27**, and **28**–**38**) were first isolated from this plant. These compounds (**1**–**38**) were evaluated for their anti-inflammatory effects on inhibiting NO production against LPS-activated microglia. Among the isolated compounds, compound **10** exhibited a slight activity (IC_{50} 23.9 μM), while compounds **18**, **30**, and **31** showed moderate activities (IC_{50} 25.3, 28.8, and 34.0 μM, respectively) to lower NO production against LPS-activated microglia, suggesting their possible role to lower neuroinflammation and neurodegenerative complications.

4. Experimental

4.1. General experimental procedures

Optical rotations and IR spectra were measured with a JASCO P-1020 polarimeter (JASCO, Easton, MD, USA) and JASCO FT/IR-4600 spectrometer (JASCO, Easton, MD, USA), respectively. UV spectra were obtained on a Shimadzu UV-1601 UV–visible spectrophotometer (Shimadzu, Tokyo, Japan). CD spectra were recorded with a JASCO J-1500 CD spectrometer (JASCO, Tokyo, Japan). NMR spectra were recorded on a Bruker AVANCE III 700 NMR spectrometer (Bruker, Karlsruhe, Germany) operating at 500 MHz (^{1}H) and 125 MHz (^{13}C). HRESI mass spectra were obtained with a Waters SYNAPT G2 (Waters, Milford, MA, USA) mass spectrometer. Semi-preparative HPLC system was conducted utilizing a Gilson 306 pump (Gilson, Middleton, WI, USA) and a Shodex refractive index detector (Shodex, New York, NY, USA) with a YMC-Triart C_{18} column (10 × 250 mm, YMC, Kyoto, Japan) at a flow rate 2 mL/min. Column chromatography was performed with silica gel 60 (70–230 and 230–400 mesh; Merck, Darmstadt, Germany) and RP-C_{18} silica gel (230–400 mesh; Merck, Darmstadt, Germany). Merck precoated silica gel F_{254} plates and RP-18 F_{254s} plates (Merck, Darmstadt, Germany) were used for TLC. Spots were detected on TLC under UV light or by heating after spraying the samples with anisaldehyde–sulfuric acid.

4.2. Plant material

The twigs of *Betula schmidtii* Regel were collected in Goesan, Korea in March 2013, and the plant was identified by one of the authors (K.R.L.). A voucher specimen (SKKU-NPL 1303) was deposited in the herbarium of the School of Pharmacy, Sungkyunkwan University, Suwon, Korea.

4.3. Extraction and isolation

The twigs of *B. schmidtii* (7.0 kg) were extracted with 80% aqueous MeOH under reflux at 70 °C for 9 h and filtered. The filtrate was concentrated under a reduced pressure to obtain a MeOH extract (410 g), which was suspended in deionized water and successively partitioned with *n*-hexane, $CHCl_3$, EtOAc, and *n*-BuOH, yielding 15 g, 18 g, 19 g, and 116 g, respectively. The *n*-BuOH-soluble layer (15 g of 116 g) was subjected to silica gel column ($CHCl_3$–MeOH–H_2O, 5:1:0.1 → 1:1:0.1) to yield five fractions (B1–B5).

Fraction B1 (2.9 g) was chromatographed on an RP-C_{18} silica gel column with 40% aqueous MeOH to give 6 subfractions (B1A–B1F). Compounds **8** (7 mg), **21** (24 mg), and **26** (20 mg) were isolated from subfractions B1A (90 mg), B1B (1.4 g), and B1C (574 mg) using semi-preparative HPLC (13–27% aqueous CH_3CN). Fraction B2 (1.3 g) was separated over an RP-C_{18} silica gel column with 30% aqueous MeOH to give 5 subfractions (B2A–B2E). Fraction B2A was fractionated by silica gel column ($CHCl_3$–MeOH–H_2O, 4:1:0.1 → 1:1:0.1) to afford three fractions (B2A1–B2A3). Fraction B2A2 (54 mg) was purified by semi-preparative HPLC (7% aqueous CH_3CN) to give compounds **5** (3 mg), **6** (3 mg), **10** (12 mg), and **12** (7 mg). Compound **7** (3 mg) was isolated from fraction B2C (217 mg) using semipreparative HPLC with 30% aqueous CH_3CN. Fraction B2D (141 mg) was separated into 4 subfractions (B2D1–B2D4) on a silica gel column, eluted with a gradient solvent system of $CHCl_3$–MeOH–H_2O (4:1:0.1 → 1:1:0.1). Compounds **15**

(4 mg), **22** (7 mg), and **25** (5 mg) were purified from subfractions B2D1 (15 mg) and B2D3 (38 mg) by semipreparative HPLC (17% aqueous CH_3CN). Fraction B3 (0.9 g) was fractionated by an RP-C_{18} silica gel column with 30% aqueous MeOH to obtain 8 subfractions (B3A–B3H). Fraction B3B (106 mg) was subjected to Lobar-A Si gel 60 (240 × 10 mm) column ($CHCl_3$–MeOH–H_2O, 3.8:1:0.1 → 1:1:0.1) to acquire 3 subfractions (B3A1–B3A3). Compounds **9** (19 mg), **16** (3 mg), and **20** (3 mg) were isolated upon purification of B3A1 (36 mg) and B3A3 (13 mg) by semipreparative HPLC (13% aqueous CH_3CN). Fraction B3C (151 mg) was separated on a Lobar-A Si gel 60 (240 × 10 mm) column ($CHCl_3$–MeOH–H_2O, 3:1:0.1) to give 3 subfractions (B3C1–B3C3). Fractions B3C1 (65 mg), B3C2 (27 mg), and B3C3 (12 mg) were purified by semipreparative HPLC (13% aqueous CH_3CN) to yield compounds **14** (30 mg) and **27** (5 mg). Compounds **17** (8 mg), **18** (4 mg), **23** (13 mg), and **29** (4 mg) were isolated upon purification of fractions B4 (27 mg), B5 (100 mg), and B6 (25 mg) through semipreparative HPLC (17–20% aqueous CH_3CN), respectively. Fraction B4 (2.6 g) was subjected to RP-C_{18} silica gel column with 20% aqueous MeOH to yield 10 subfractions (B4A–B3J). B4B (82 mg) was separated to silica gel column ($CHCl_3$–MeOH–H_2O, 3:1:0.1) to afford 2 subfractions (B4A–B4B) and further purified by semipreparative HPLC (6% aqueous CH_3CN) to afford **2** (5 mg), **4** (5 mg), **11** (7 mg), and **13** (4 mg), respectively. B4D (104 mg) was purified to give **3** (3 mg) and **35** (5 mg) by semipreparative HPLC (12% aqueous CH_3CN) after fractionation on a Lobar-A Si gel 60 (240 × 10 mm) column ($CHCl_3$–MeOH–H_2O, 2:1:0.1). Fractions B4E (100 mg) and B4G (159 mg) were purified by semipreparative HPLC (9–20% aqueous CH_3CN) to acquire compounds **33** (3 mg) and **28** (9 mg), respectively.

The EtOAc-soluble layer (11 g of 19 g) was chromatographed on a silica gel column (EtOAc-MeOH-H_2O, 10:1:0.1 → 1:1:0.1) to yield 3 fractions (E1–E3). Fraction E1 (5.4 g) was further separated over a silica gel column ($CHCl_3$–MeOH–H_2O, 6:1:0.1 → 1:1:0.1) to obtain 9 fractions (E1A–E1I). Fraction E1E (117 mg) was subjected to passage over a Lobar-A RP-C_{18} (240 × 10 mm) column with 40% aqueous MeOH and further purified by semipreparative HPLC (20% aqueous CH_3CN) to give compound **1** (5 mg). Fraction E1F (1.4 g) was separated over an RP-C_{18} silica gel column with 50% aqueous MeOH to give 5 subfractions (E1F1–E1F5). Compounds **19** (5 mg), **32** (32 mg), and **34** (5 mg) were purified from fraction E1F3 (949 mg) by semipreparative HPLC (30% aqueous CH_3CN). Compounds **36** (18 mg) and **37** (4 mg) were obtained by purifying fraction E1G (260 mg) through semipreparative HPLC (12% aqueous CH_3CN) after separation over an RP-C_{18} silica gel column with 40% aqueous MeOH. Fraction E1H (734 mg) was fractionated over an RP-C_{18} silica gel column with 35% aqueous MeOH to give 3 subfractions (E1H1–E1H3) and further purified by semipreparative HPLC (17% aqueous CH_3CN) to yield compound **38** (12 mg). Fraction E2 (0.7 g) was separated on an RP-C_{18} silica gel column with 40% aqueous MeOH resulting in 7 subfractions (E2A–E2G). Fraction E2E (101 mg) was subjected to passage over a Lobar-A Si gel 60 (240 × 10 mm) column ($CHCl_3$–MeOH–H_2O, 5:1:0.1) to obtain 4 subfractions (E2E1–E2E4). Compounds **30** (4 mg) and **31** (8 mg) were isolated by purifying subfraction B2E2 (20 mg) through semipreparative HPLC (28% aqueous CH_3CN). Fraction E3 (1.8 g) was chromatographed on an RP-C_{18} silica gel column with 40% aqueous MeOH to give 6 subfractions (E3A–E3F). The subfraction E3B (1.2 g) was purified by semipreparative HPLC (17% aqueous CH_3CN) to yield compound **24** (8 mg).

4.3.1. 3,5-Dihydroxyphenyl-(6′-O-benzoyl)-1-O-β-D-glucopyranoside (1)

Colorless gum; $[\alpha]_D^{25}$–56.5 (*c* 0.10, MeOH); UV (MeOH) λ_{max} (log ε) 272 (2.23), 226 (3.13), 205 (3.54) nm; IR (KBr) ν_{max} cm^{-1}: 3702, 3670, 3394, 2970, 2868, 2835, 1351, 1054, 1022; ^1H NMR (CD_3OD, 500 MHz) and ^{13}C NMR (CD_3OD, 125 MHz) data, see Table 1; HRESIMS (positive-ion mode) *m/z* 415.1004 $[M + Na]^+$ (calcd. for $C_{19}H_{20}O_9Na$, 415.1005).

4.3.2. (7R,8R)-1-(4-hydroxy-3-methoxyphenyl)propan-7,8-diol-4-O-β-D-apiofuranosyl-(1 → 6)-O-β-D-glucopyranoside (2)

Colorless gum; $[\alpha]_D^{25}$–107.9 (*c* 0.10, MeOH); UV (MeOH) λ_{max} (log ε) 276 (2.42), 226 (2.96), 202 (3.50) nm; IR (KBr) ν_{max} cm^{-1}: 3702, 3670, 3399, 2956, 2868, 2835, 1352, 1054, 1011; ^1H NMR (CD_3OD, 500 MHz) and ^{13}C NMR (CD_3OD, 125 MHz) data, see Table 1; HRESIMS (positive-ion mode) *m/z* 515.1735 $[M + Na]^+$ (calcd. for $C_{21}H_{32}O_{13}Na$, 515.1741).

4.3.3. 4-Hydroxy-1-(2-hydroxyethyl)phenyl-3-O-β-D-apiofuranosyl-(1 → 6)-O-β-D-glucopyranoside (3)

Colorless gum; $[\alpha]_D^{25}$–78.3 (*c* 0.10, MeOH); UV (MeOH) λ_{max} (log ε) 279 (2.44), 222 (sh), 201 (3.37) nm; IR (KBr) ν_{max} cm^{-1}: 3703, 3670, 3492, 3398, 2961, 2868, 2835, 1351, 1054, 1012; ^1H NMR (CD_3OD, 500 MHz) and ^{13}C NMR (CD_3OD, 125 MHz) data, see Table 1; HRESIMS (positive-ion mode) *m/z* 471.1473 $[M + Na]^+$ (calcd. for $C_{19}H_{28}O_{12}Na$, 471.1478).

4.3.4. 3,5-Dihydroxy-1-(hydroxymethyl)phenyl-4-O-β-D-apiofuranosyl-(1 → 6)-O-β-D-glucopyranoside (4)

Colorless gum; $[\alpha]_D^{25}$–17.7 (*c* 0.10, MeOH); UV (MeOH) λ_{max} (log ε) 274 (2.08), 226 (sh), 203 (3.35) nm; IR (KBr) ν_{max} cm^{-1}: 3702, 3669, 3491, 3397, 2970, 2946, 2868, 2835, 1352, 1054, 1022; ^1H NMR (CD_3OD, 500 MHz) and ^{13}C NMR (CD_3OD, 125 MHz) data, see Table 1; HRESIMS (positive-ion mode) *m/z* 473.1267 $[M + Na]^+$ (calcd. for $C_{18}H_{26}O_{13}Na$, 473.1271).

4.3.5. (+)-(8R,7′S,8′R)-6-O-β-D-glucopyranosyl lyoniresinol-9′-O-β-D-xylopyranoside (20)

Colorless gum; $[\alpha]_D^{25}$ +13.2 (*c* 0.10, MeOH); UV (MeOH) λ_{max} (log ε) 276 (3.82), 230 (sh), 208 (4.13) nm; CD (MeOH) λ_{max} ($\Delta\varepsilon$) 287 (−2.75), 272 (+4.39), 241 (+5.52), 222 (−3.25); IR (KBr) ν_{max} cm^{-1}: 3702, 3670, 3400, 2959, 2868, 2835, 1351, 1054, 1011; ^1H NMR (CD_3OD, 500 MHz) and ^{13}C NMR (CD_3OD, 125 MHz) data, see Table 2; HRESIMS (positive-ion mode) *m/z* 737.2625 $[M + Na]^+$ (calcd. for $C_{33}H_{46}O_{17}Na$, 737.2633).

4.3.6. Orobol-7-O-α-L-rhamnopyranosyl-(1 → 6)-O-β-D-glucopyranoside (28)

Colorless gum; $[\alpha]_D^{25}$–61.1 (*c* 0.10, MeOH); UV (MeOH) λ_{max} (log ε) 290 (sh), 262 (3.66), 205 (3.91) nm; IR (KBr) ν_{max} cm^{-1}: 3702, 3670, 3492, 3396, 2970, 2946, 2868, 2835, 1351, 1054, 1022; ^1H NMR (CD_3OD, 500 MHz) and ^{13}C NMR (CD_3OD, 125 MHz) data, see Table 2; HRESIMS (positive-ion mode) *m/z* 617.1479 $[M + Na]^+$ (calcd. for $C_{27}H_{30}O_{15}Na$, 617.1482).

4.4. Acid hydrolysis of compounds 1–4, 20, and 28

Compounds **1**–**4**, **20**, and **28** (each 1.0 mg) were hydrolyzed with 1 N HCl (1 mL) under reflux for 2 h at 90 °C. The hydrolysate was diluted with H_2O and extracted with EtOAc. The organic layer was removed under reduced pressure to give aglycone (**2a**–**4a**, **20a**, and **28a**), respectively.

4.4.1. (7R,8R)-1-(4-hydroxy-3-methoxyphenyl)propan-7,8-diol (2a)

Brownish gum; $[\alpha]_D^{25}$–47.4 (*c* 0.05, MeOH); ^1H NMR (CD_3OD, 700 MHz) δ 6.78 (1H, d, J = 1.9 Hz), 6.75 (1H, d, J = 8.0 Hz), 6.65 (1H, dd, J = 8.0, 1.9 Hz), 3.91 (1H, d, J = 6.8 Hz), 3.65 (1H, overlap), 0.90 (3H, d, J = 7.2 Hz).

4.4.2. 4-Hydroxy-1-(2-hydroxyethyl)phenol (3a)

Brownish gum; ^1H NMR (CD_3OD, 700 MHz) δ 6.69 (1H, d, J = 8.0 Hz), 6.67 (1H, d, J = 2.0 Hz), 6.54 (1H, dd, J = 8.0, 2.0 Hz), 3.69 (2H, t, J = 7.3 Hz), 2.68 (2H, t, J = 7.3 Hz).

4.4.3. 3,5-Dihydroxy-1-(hydroxymethyl)phenol (**4a**)

Brownish gum; ^{1}H NMR (CD_3OD, 700 MHz) δ 6.45 (2H, s), 4.49 (2H, s).

4.4.4. (+)-lyoniresinol (**20a** = **23**)

Brownish gum; $[\alpha]_D^{25}$ +58.2 (*c* 0.03, MeOH); ^{1}H NMR (CD_3OD, 700 MHz) δ 6.59 (1H, s), 6.38 (2H, s), 4.31 (1H, d, J = 5.6 Hz), 3.86 (3H, s), 3.85 (1H, overlap), 3.74 (6H, s), 3.60 (1H, dd, J = 10.9, 5.1 Hz), 3.49 (2H, overlap), 3.38 (3H, s), 2.70 (1H, dd, J = 15.4, 4.7 Hz), 2.58 (1H, dd, J = 15.4, 11.6 Hz), 1.97 (1H, m), 1.63 (1H, m).

4.4.5. Orobol (**28a**)

Brownish gum; ^{1}H NMR (CD_3OD, 700 MHz) δ 8.06 (1H, s), 7.04 (1H, d, J = 2.0 Hz), 6.87 (1H, dd, J = 8.1, 2.0 Hz), 6.84 (1H, d, J = 8.1 Hz), 6.36 (1H, d, J = 2.2 Hz), 6.24 (1H, d, J = 2.2 Hz).

4.5. Determination of absolute configuration of sugar moieties of compounds **1**–**4**, **20**, and **28**

The aqueous layer, obtained after the separation of organic layer, was neutralized through an Amberlite IRA-67 column and repeatedly evaporated to obtain each sugar fraction. The sugar residue was dissolved in anhydrous pyridine (0.5 mL) followed by adding 2.0 mg of L-cysteine methyl ester hydrochloride. The mixture was stirred at 60 °C for 1.5 h. Then, 0.1 mL of 1-trimethylsilylimidazole was added and the mixture was stirred at 60 °C for another 2 h. Finally, the mixture was partitioned between *n*-hexane and H_2O (1.0 mL each) and the organic layer (1.0 μL) was analyzed by GC/MS under the following conditions: column temperature, 230 °C; injection temperature, 250 °C; carrier gas, He gas; flow rate 1.0 mL/min. D-Glucose, D-apiose, D-xylose, and L-rhamnose were confirmed by co-injection of the hydrolysate with standard silylated samples, giving single peaks at D-glucose (11.471 min) for **1**, D-glucose and D-apiose (11.467 min and 9.264 min) for **2**, D-glucose and D-apiose (11.468 min and 9.262 min) for **3**, D-glucose and D-apiose (11.467 min and 9.259 min) for **4**, D-glucose and D-xylose (11.465 min and 9.340 min) for **20**, and D-glucose and L-rhamnose (11.471 min and 10.002 min) for **28**, respectively. Authentic samples of D-glucose, D-apiose, D-xylose, and L-rhamnose treated in the same way showed retention times of 11.468, 9.261, 9.345, and 10.008 min, respectively.

4.6. NO production and cell viability assay in LPS-activated BV-2 cells

BV-2 cells were used as the representative cell line of CNS-microglia to evaluate the anti-inflammatory effect of isolated compounds (Subedi et al., 2019a,). BV-2 cells were seeded in a 96-well plate at the density of 4×10^4 cells/well and incubated overnight. Seeded cells were pre-treated with or without compounds and after 30 min LPS (100 ng/ml)-activation was performed and the plate were incubated for 24 h. Nitrite (NO_2, a soluble oxidation product of NO) concentrations present in the culture medium (CM) were measured using the Griess reagent (0.1% *N*-1-naphthylethylenediamine dihydrochloride and 1% sulfanilamide in 5% phosphoric acid). The supernatant (50 μL) from each well was transferred to a new 96 well plate and it was mixed with an equal volume of Griess reagent. After 10 min, the absorbance was measured at 570 nm using microplate reader (Emax, Molecular Devices, Sunnyvale, CA, USA). Graded sodium nitrite solution was used as a standard to gauge the NO_2 concentration. Cell viability was performed as described previously with slight modification (, 2019b). After transferring the 50 μL of CM from treated plate for NO measurement, remaining CM in the plate were removed by suction and the attached/live cells were incubated with 3-(4,5-dimethylthiazol-2-yl)-2,5-diphenyl-tetrazolium bromide (MTT) solution making the final concentration 0.5 mg/ml and kept the plate in incubated in a humidified incubator with 5% CO_2 at 37 °C with complete light protection for an hour. MTT solution was removed and the blue stained cells were exposed with almost 200 μL of DMSO, the blue stained live cells were converted to purple color formazan and this color change was quantified by measuring the absorbance at 570 nm in a microplate reader. Cell viability was measured as % of only LPS treated group where LPS treated group were set as 100%. The NO synthase inhibitor N^G-monomethyl-L-arginine (L-NMMA) was used as a positive control.

Acknowledgements

This research was supported by the Basic Science Research Program through the National Research Foundation of Korea (NRF) funded by the Ministry of Education, Science and Technology (2016R1A2B2008380). We thank the Korea Basic Science Institute for the MS spectrometric analysis.

Appendix A. Supplementary data

Supplementary data to this article can be found online at https://doi.org/10.1016/j.phytochem.2019.112085.

References

Abdel Kader Ahmed, S., Al-Refai, M., 2014. Chemical constituents and cytotoxic activities of the extracts of *Melilotus indicus*. Eur. J. Chem. 5, 503–506.
Achenbach, H., Loewel, M., Waibel, R., Gupta, M., Solis, P., 1992. New lignan glucosides from *Stemmadenia minima*. Planta Med. 58, 270–272.
Anhut, S., Zinsmeister, H.D., Mues, R., Barz, W., Mackenbrock, K., Koester, J., Markham, K.R., 1984. The first identification of isoflavones from a bryophyte. Phytochemistry 23, 1073–1075.
Backheet, E.Y., Farag, S.F., Ahmed, A.S., Sayed, H.M., 2003. Flavonoids and cyanogenic glycosides from the leaves and stem bark of *Prunus persica* (L.) Batsch (Meet Ghamr) peach local cultivar in Assiut region. Bull. Pharmaceut. Sci. 26, 55–66.
Balboul, B.A.A.A., Ahmed, A.A., Otsuka, H., De Adams, A., 1996. 4-Hydroxyphenylpropan-7,8-diols and derivatives from *Narvalina domingensis*. Phytochemistry 42, 1191–1193.
Cui, C.B., Tezuka, Y., Kikuchi, T., Nakano, H., Tamaoki, T., Park, J.H., 1992a. Constituents of a fern, *Davallia mariesii* Moore. II. Identification and proton and carbon-13 nuclear magnetic resonance spectra of procyanidin B-5, epicatechin-(4β→8)-epicatechin-(4β→6)-epicatechin, and epicatechin-(4β→6)-epicatechin-(4β→8)-epicatechin-(4β→6)-epicatechin. Chem. Pharm. Bull. 40, 889–898.
Cui, C.B., Tezuka, Y., Kikuchi, T., Nakano, H., Tamaoki, T., Park, J.H., 1992b. Constituents of a fern, *Davallia mariessi* Moore. IV. Isolation and structures of a novel norcarotane sesquiterpene glycoside, a chromone glucuronide, and two epicatechin glycosides. Chem. Pharm. Bull. 40, 2035–2040.
Fu, H.-Z., Yang, J.-Z., Li, C.-J., Zhang, D.-M., 2011. A new benzophenone glycoside from the leaves of *Psidium guajava* L. Chin. Chem. Lett. 22, 178–180.
Fuchino, H., Satoh, T., Hida, J., Terada, M., Tanaka, N., 1998. Chemical evaluation of *Betula* species in Japan. VI. Constituents of *Betula schmidtii*. Chem. Pharm. Bull. 46, 1051–1053.
Fuchino, H., Satoh, T., Tanaka, N., 1995. Chemical evaluation of *Betula* species in Japan. I. Constituents of *Betula ermanii*. Chem. Pharm. Bull. 43, 1937–1942.
Gan, M., Zhang, Y., Lin, S., Liu, M., Song, W., Zi, J., Yang, Y., Fan, X., Shi, J., Hu, J., Sun, J., Chen, N., 2008. Glycosides from the root of *Iodes cirrhosa*. J. Nat. Prod. 71, 647–654.
Geibel, M., Geiger, H., Treutter, D., 1990. Tectochrysin 5- and genistein 5-glucosides from the bark of *Prunus cerasus*. Phytochemistry 29, 1351–1353.
Gelders, G., Baekelandt, V., Van der Perren, A., 2018. Linking neuroinflammation and neurodegeneration in Parkinson's disease. J. Immunol. Res. https://doi.org/10.1155/2018/4784268.
Hara, S., Okabe, H., Mihashi, K., 1987. Gas-liquid chromatographic separation of aldose enantiomers as trimethylsilyl ethers of methyl 2-(polyhydroxyalkyl)thiazolidine-4(R)-carboxylates. Chem. Pharm. Bull. 35, 501–506.
Itoh, A., Tanaka, Y., Nagakura, N., Akita, T., Nishi, T., Tanahashi, T., 2008. Phenolic and iridoid glycosides from *Strychnos axillaris*. Phytochemistry 69, 1208–1214.
Kanchanapoom, T., Kasai, R., Yamasaki, K., 2002. Iridoid and phenolic diglycosides from *Canthium berberidifolium*. Phytochemistry 61, 461–464.
Kanho, H., Yaoya, S., Kawahara, N., Nakane, T., Takase, Y., Masuda, K., Kuroyanagi, M., 2005. Biotransformation of benzaldehyde-type and acetophenone-type derivatives by *Pharbitis nil* hairy roots. Chem. Pharm. Bull. 53, 361–365.
Kawahara, E., Fujii, M., Kato, K., Ida, Y., Akita, H., 2005. Chemoenzymatic synthesis of naturally occurring benzyl 6-*O*-glycosyl-*β*-D-glucopyranosides. Chem. Pharm. Bull. 53, 1058–1061.
Khalid, S.A., Gellert, M., Szendrei, K., Duddeck, H., 1989. Prunetin 5-*O*-*β*-D-glucopyranoside, an isoflavone from the peduncle of *Prunus avium* and *P. cerasus*. Phytochemistry 28, 1560–1561.
Kim, C.S., Subedi, L., Park, K.J., Kim, S.Y., Choi, S.U., Kim, K.H., Lee, K.R., 2015. Salicin derivatives from *Salix glandulosa* and their biological activities. Fitoterapia 106, 147–152.
Kitajima, J., Ishikawa, T., Tanaka, Y., Ono, M., Ito, Y., Nohara, T., 1998. Water-soluble

constituents of fennel. V. Glycosides of aromatic compounds. Chem. Pharm. Bull. 46, 1587–1590.
Kitajima, J., Kamoshita, A., Ishikawa, T., Takano, A., Fukuda, T., Isoda, S., Ida, Y., 2003. Glycosides of *Atractylodes japonica*. Chem. Pharm. Bull. 51, 152–157.
Laupattarakasem, P., Houghton, P.J., Hoult, J.R.S., 2004. Anti-inflammatory isoflavonoids from the stems of *Derris scandens*. Planta Med. 70, 496–501.
Le, H.T., Ha, D.T., Minh, C.T.A., Kim, T.H., Kiem, P.V., Nguyen, D.T., Na, M.K., 2012. Constituents from the stem barks of *Canarium bengalense* with cytoprotective activity against hydrogen peroxide-induced hepatotoxicity. Arch Pharm. Res. (Seoul) 35, 87–92.
Lee, A.-L., Ley, S.V., 2003. The synthesis of the anti-malarial natural product polysphorin and analogues using polymer-supported reagents and scavengers. Org. Biomol. Chem. 1, 3957–3966.
Lee, D.G., Jung, H.J., Woo, E.-R., 2005. Antimicrobial property of (+)-lyoniresinol-3α-*O*-β-D-glucopyranoside isolated from the root bark of *Lycium chinense* Miller against human pathogenic microorganisms. Arch Pharm. Res. (Seoul) 28, 1031–1036.
Lei, Y., Wu, L.-J., Shi, H.-M., Tu, P.-F., 2008. Three new glycosides from the stems of *Miliusa balansae*. Helv. Chim. Acta 91, 495–500.
Li, L., Seeram, N.P., 2010. Maple syrup phytochemicals include lignans, coumarins, a stilbene, and other previously unreported antioxidant phenolic compounds. J. Agric. Food Chem. 58, 11673–11679.
Lou, H., Yamazaki, Y., Sasaki, T., Uchida, M., Tanaka, H., Oka, S., 1999. A-type proanthocyanidins from peanut skins. Phytochemistry 51, 297–308.
Lull, M.E., Block, M.L., 2010. Microglial activation and chronic neurodegeneration. Neurotherapeutics 7, 354–365.
Ma, J., Jin, X., Yang, L., Liu, Z.-L., 2004. Diarylheptanoids from the rhizomes of *Zingiber officinale*. Phytochemistry 65, 1137–1143.
Matsuoka, N., Ikeda, T., El-Aasr, M., Manabe, H., Murakami, Y., Deguchi, H., Nohara, T., 2011. Study of the chemical constituents of *Pruni Cortex* and its related parts. J. Nat. Med. 65, 166–171.
Park, K.J., Subedi, L., Kim, S.Y., Choi, S.U., Lee, K.R., 2018. Bioactive triterpenoids from twigs of *Betula schmidtii*. Bioorg. Chem. 77, 527–533.
Raab, T., Barron, D., Vera, F.A., Crespy, V., Oliveira, M., Williamson, G., 2010. Catechin glucosides: occurrence, synthesis, and stability. J. Agric. Food Chem. 58, 2138–2149.
Rastogi, S., Pandey, M.M., Kumar Singh Rawat, A., 2015. Medicinal plants of the genus *Betula*-Traditional uses and a phytochemical-pharmacological review. J. Ethnopharmacol. 159, 62–83.
Seigler, D.S., Pauli, G.F., Nahrstedt, A., Leen, R., 2002. Cyanogenic allosides and glucosides from *Passiflora edulis* and *Carica papaya*. Phytochemistry 60, 873–882.
Smite, E., Pan, H., Lundgren, L.N., 1995. Lignan glycosides from inner bark of *Betula pendula*. Phytochemistry 40, 341–343.
Subedi, L., Cho, K., Park, Y.U., Choi, H.J., Kim, S.Y., 2019a. Sulforaphane-enriched broccoli sprouts pretreated by pulsed electric fields reduces neuroinflammation and ameliorates scopolamine-induced amnesia in mouse brain through its antioxidant ability via Nrf2-HO-1 activation. Oxid. Med. Cell. Longev. https://doi.org/10.1155/2019/3549274.
Subedi, L., Lee, J.H., Yumnam, S., Ji, E., Kim, S.Y., 2019b. Anti-inflammatory effect of sulforaphane on LPS-activated microglia potentially through JNK/AP-1/NF-κB inhibition and Nrf2/HO-1 activation. Cells 8. https://doi.org/10.3390/cells8020194.
Suh, W.S., Kim, K.H., Kim, H.K., Choi, S.U., Lee, K.R., 2015. Three new lignan derivatives from *Lindera glauca* (SIEBOLD et ZUCC.) BLUME. Helv. Chim. Acta 98, 1087–1094.
Suzuki, Y., Yamaguchi, I., Murofushi, N., Takahashi, N., Sugawara, F., Yoshida, S., Nukada, T., Ogawa, T., 1988. Synthesis of benzyl 6-*O*-β-D-apiofuranosyl-β-*D*-glucopyranoside, a metabolite of benzoic acid in *Lemna paucicostata*. Agric. Biol. Chem. 52, 1261–1266.
Verotta, L., Orsini, F., Pelizzoni, F., Torri, G., Rogers, C.B., 1999. Polyphenolic glycosides from african proteaceae. J. Nat. Prod. 62, 1526–1531.
Yamauchi, H., Kakuda, R., Yaoita, Y., Machida, K., Kikuchi, M., 2007. Two new glycosides from the whole plants of *Glechoma hederacea*. L. Chem. Pharm. Bull. 55, 346–347.
Yoshinari, K., Sashida, Y., Shimomura, H., 1989. Two new lignan xylosides from the barks of *Prunus ssiori* and *Prunus padus*. Chem. Pharm. Bull. 37, 3301–3303.
Yuste, J.E., Tarragon, E., Campuzano, C.M., Ros-Bernal, F., 2015. Implications of glial nitric oxide in neurodegenerative diseases. Front. Cell. Neurosci. 9. https://doi.org/10.3389/fncel.2015.00322.
Zhong, X.-N., Otsuka, H., Ide, T., Hirata, E., Takeda, Y., 1999. Hydroquinone diglycoside acyl esters from the leaves of *Myrsine seguinii*. Phytochemistry 52, 923–927.